Humping mechanisms present in high speed welding

E. Soderstrom* and P. Mendez

As welding speeds continually increase owing to automation and newer processes, a common defect that occurs is humping. Humping is the periodic occurrence of beadlike protuberances. The objective of the present investigation is to review current and previous researches that were made on humping, including both experimental and theoretical studies. It is found that humping can be classified into two distinct categories of formation: gouging region morphology and beaded cylinder morphology. Various theories that explain the two types of humping formation are examined. Experimental data compiled from many sources are presented to verify the models and explain the fundamental mechanisms of humping morphology. Humping prevention measures that can be applied directly to industrial fabrication are also included. The direct benefit is increased travel speeds that reduce production costs.

Keywords: Humping, Beading, Undercutting, Defect formation, High speed welding

Introduction

Throughout the world in the past several decades, a significant increase in the use of automated welding machines has been realised. In many production applications, these machines have better efficiencies, superior repeatability and increased production rates as compared with manual welding operators. Because heat intensities increased with newer processes such as laser and electron beam welding, the travel speeds increased as well.[1] As manufacturers strive to reduce production costs, many have tried to increase welding production by increasing the welding speed. One would think that as further advancements were made in automated welding controls, weld quality would continue to improve. However, one of the problems that arise from increased travel speed is commonly referred to as humping.

The humping phenomenon has been the focus of many research papers published in the past 35 years. As will be shown, humping has been reported in several different welding processes. Bradstreet[2] is credited with publishing the first paper to directly recognise humping during GMAW. Since then, humping has been observed in GTAW,[3–5] submerged arc welding (SAW),[6,7] laser welding,[8,9] electron beam welding[10,11] and is even evident in other fields such as digital microfabrication using waxes.[12] Throughout these studies, different controlling variables have been identified, including welding atmosphere, metal composition, surface condition and heat input. All of these have an influence on defect formation. The liquid metal flow of the weld pool has also been observed to contribute significantly to the onset of humping. Variables related to the welding arc include current, arc length, shielding gas, electrode angle and electrode geometry. Undercutting, a common weld defect not limited to high speed welding, has been observed to occur in association with humping and evidence exists that similar mechanisms are at work in both undercutting and humping.

As researchers have exposed how the different variables influence the humping phenomenon through experimental observations, others have proposed various theories of why humping occurs and the fundamental mechanisms of formation. Bradstreet[2] proposed a liquid instability theory that was later modified by Gratzke[9] explaining humping during GMA and laser welding. Yamamoto[5] used the theory of hydraulic jump to account for the humping phenomenon. Mills and Keene[13] theorised that humping was owing to the Marangoni flow in the weld pool. Lin[14,15] explained humping by a compound vortex theory based on electrically driven rotational flow in the weld pool. Most recently, Mendez[3] proposed a theory of arc induced humping based on the pressure and heating ranges of the arc, similar to the model proposed by Paton.[7] Kumar and DebRoy[16] have proposed a theory for the onset of humping based on the Kelvin-Helmholtz instability of a free surface.

The purpose of the present paper is to review current and previous researches on the topic of humping within the framework of two distinct humping morphologies: gouging region morphology (GRM) and beaded cylinder morphology (BCM). This review includes both experimental observations and theories of the proposed mechanisms of formation for several welding processes and base materials. The two main humping morphologies will be analysed by discussing their appearances as seen through experimental observations and theories that have been developed to describe them. Finally,

Colorado School of Mines, 1500 Illinois St., Room HH 280, Golden, CO 80401, USA

*Corresponding author, email esoderst@mines.edu

Published by Maney on behalf of the Institute
Received 15 May 2006; accepted 19 June 2006
DOI 10.1179/174329306X120787

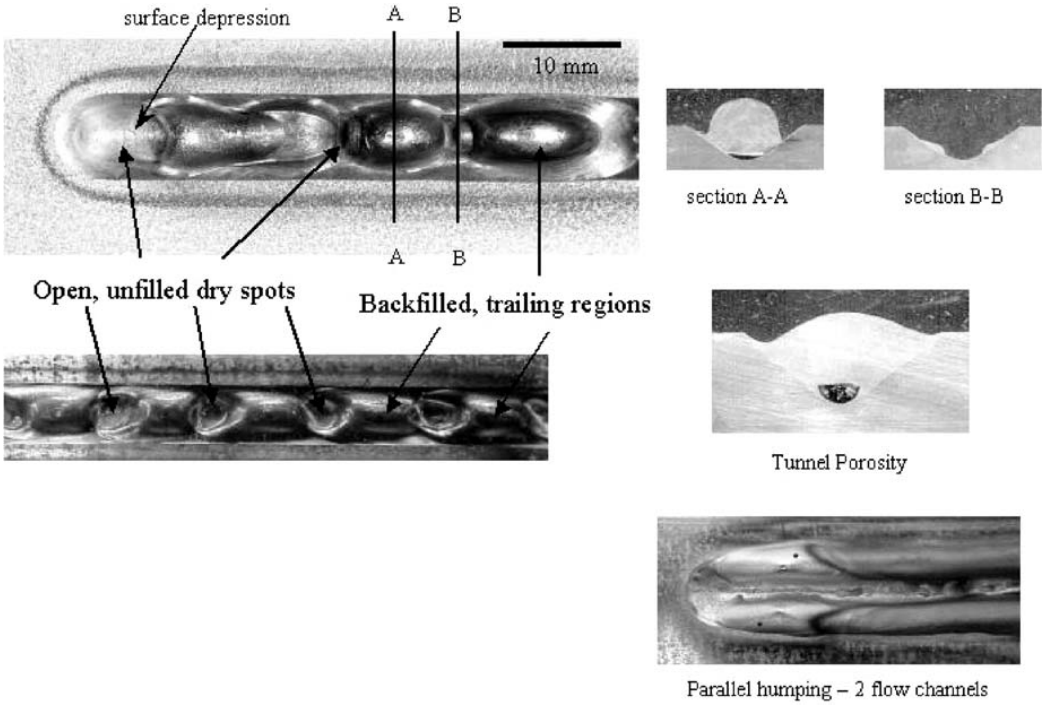

1 Several defects that illustrate humping by GRM during GTAW: note all defects exhibit unfilled dry spots and severe surface depressions

combining the framework of analysis with published observations, the authors present suggestions for the prevention of humping and its related defects.

Morphology of humping defect

Initially, humped welds appear to have a very random morphology; however, detailed observation shows that all humped welds can be clustered into two distinctive classifications. In some uncommon cases, welds might present features of both morphologies simultaneously. The two classifications are directly linked to the GRM or to the BCM, which will be shown below. Therefore, both GRM and BCM will be termed as appropriate.

Typical GRM defects are shown in Fig. 1. All of these welds were made using the GTA process at high currents and high travel speeds. This morphology is characterised by open, unfilled dry spots in between the humped beads. Besides, the front of the weld pool exhibits a very large depression known as the gouging region. The bulk of the molten metal, which is called the trailing region, resides in the back of the weld pool. In some cases, two small channels appear at the walls of the gouging region. Other defects that share similarity with this humping mechanism are tunnel porosities, in which the gouging region extends under the surface of the weld and split bead welds, where the gouging region splits the weld bead longitudinally.

Figure 2 is a similar compilation of images that show BCM defects. It is evident that this type of humping is noticeably different from what is shown in Fig. 1. Not only are the characteristic dry spots missing, but also the welds show no evidence of depressions below the workpiece surface. The distinguishing features of BCM include beadlike protuberances that sit above the surface of the workpiece and are connected by a narrow central channel. The weld bead in this case has a continuous undulating aspect. In some cases of disconnected protuberances, traces of a central channel can still be observed.

Figure 3 includes a series of hybrid defects that have qualities of both the GRM and the BCM. Figure 3*a–c* is taken from Nguyen[17] that depicts humping during GMAW. A deeply depressed surface is apparent, but the image shows no evidence of an unfilled dry spot. The dominating method for humping in this situation is the BCM because of the long liquid weld pool that is formed. Two examples of split bead humping are shown in Fig. 3*d*, which are similar to the parallel humping image shown in Fig. 1, however, the two flow channels become long enough to exhibit BCM. The driving mechanism in this case is the GRM because of the existence of the gouging region. Figure 3*e*, from Bradstreet,[2] is another example of combined defect formation during GMAW. In the region directly under

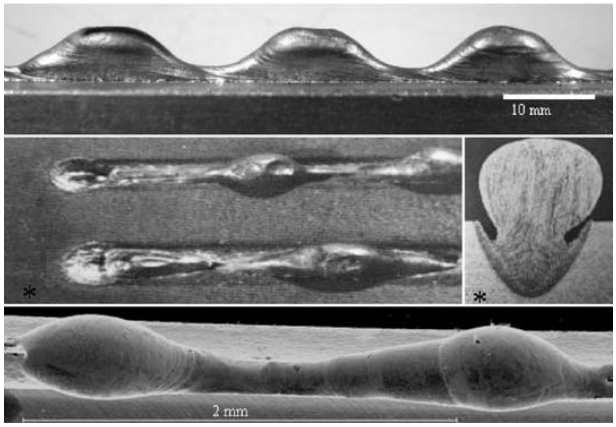

2 Several defects that form resulting from BCM: all defects form series of beaded protuberances that sit above plate surface; images marked with * are taken from Bradstreet[2]

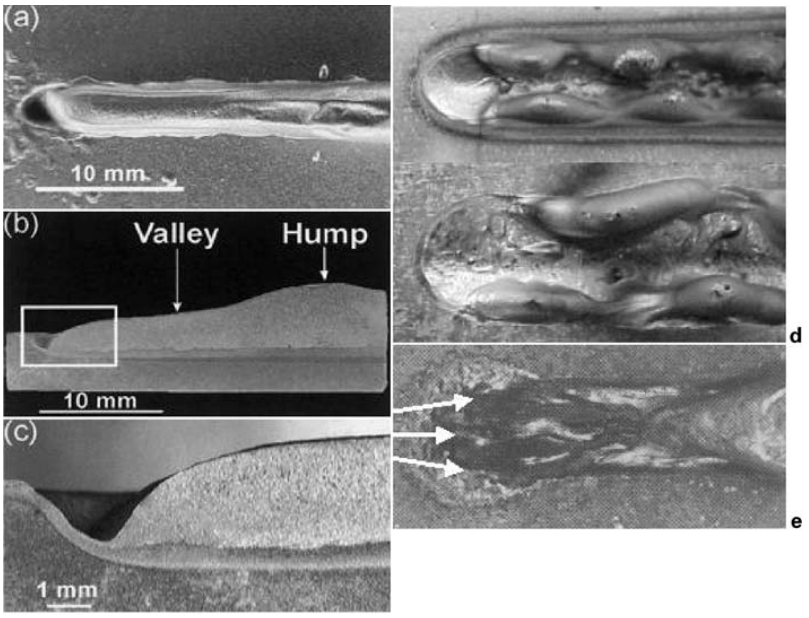

a–c humping in GMAW from Nguyen;[16] *d* split bead humping in GTAW; *e* three separate flow channels in GTAW from Bradstreet[2]

3 Several images of hybrid defects containing attributes from both GRM (Fig. 1) and BCM (Fig. 2)

the arc, three flow channels separated by two 'dry' regions can be identified, which is a feature of the GRM. The two outermost channels are formed from the melted base metal, whereas the central channel originates from the liquid filler metal. Directly behind this depressed region, the three channels combine and form a long liquid weld pool that humps by BCM.

Theoretical models

In this section, five theories that attempt to explain humping formation are reviewed. Several of them are specifically aimed at one type of humping morphology (compound vortex, hydraulic jump and arc induced aim at GRM and capillary instability aims at BCM) while the Marangoni approach does not define a target morphology. The newest approach to humping by Kumar and DebRoy described at 2005 AWS/Fabtec conference is not included in this review.

Marangoni model

Mills and Keene,[13] reviewing the factors affecting weld penetration in their paper, suggested that humping and undercutting could be attributed to Marangoni forces created in the weld pool. This suggestion is based on their observation that humping is affected by sulphur content in the weld metal. They did not provide a detailed description of the morphology addressed, but their analysis of Marangoni recirculating flows in the weld pool would be consistent with BCM instead of GRM. Owing to the gradient in temperature found throughout the weld pool, a similar gradient in surface tension is created. As a result, thermocapillary flow is initiated in the molten metal. Figure 4 shows the predicted weld metal flow owing to the effects of Marangoni forces. Depending on a number of welding parameters, this convective flow may be directed inward or outward and can have a significant effect on weld penetration. Figure 4*a* shows that an inward flow pattern would create a raised free surface along with a region of undercut near the edges of the weld pool. Mills and Keene speculated that the raised free surface could be a precursor of the humped bead.

Compound vortex model

Lin and Eagar[14,15] presented an arc model that combines a compound vortex to explain the increase in penetration depth with the current observed during high current GTAW. Using this compound vortex hypothesis, they also attempted to explain the formation of humping. The proposed mechanism for vortex formation is based on surface tension and electromagnetic forces. It is stated in their model that as the hump is formed, it attracts more current from the arc. This attraction shifts the arc towards the rear of the weld pool. This rearward shift of the arc, coupled with the flow of metal, creates the hump and subsequently the arc redirects itself forward and the process continues. This unsteady motion is used to explain defect formation. This model attempts to explain humping formation in the deep penetration regime, which is owing to the action of the arc over the gouging region; therefore, it addresses the GRM. No further experiments have been performed to confirm the presence of the vortex, and this model has not been pursued further in the literature.

Hydraulic jump model

Yamamoto[5] approached the humping problem from a fluid dynamics standpoint and modelled it after the

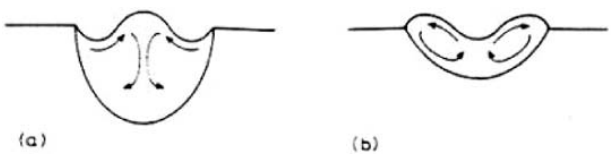

a inward surface flows with downward flow in centre; *b* outward surface flows with downward flow at periphery of weld pool

4 Predicted surface profiles owing to Marangoni flow[13]

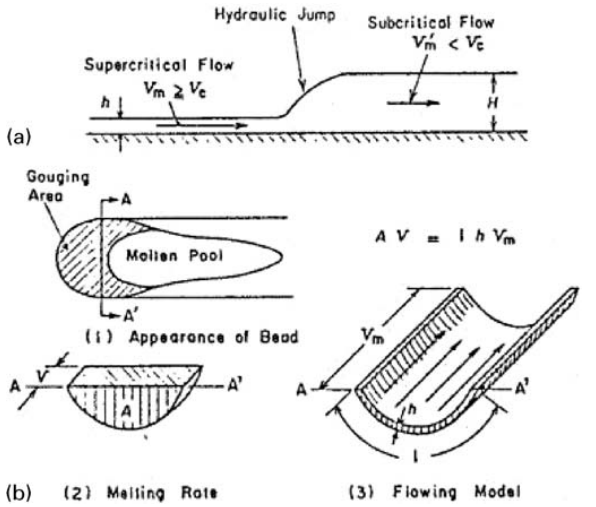

a model of hydraulic jump; *b* analytical model of gouging region

5 Model of hydraulic jump and gouging region[5]

event known as hydraulic jump. Figure 5 is the schematic model of hydraulic jump that Yamamoto used to explain humping. In Fig. 5*a*, the region of supercritical flow before the jump is compared with the thin layer of molten metal produced before the onset of humping, indicating that this model aims at predicting the GRM. Similarly, the jump and ensuing subcritical flow region resembles the humped region formed during high speed GTAW welding. The other parameters used for predicting the melting rate and flow model are set forth in Fig. 5*b*. From experimental observations, parameters used to calculate the supercritical velocity can be deduced and the resulting values meet the criteria for hydraulic jump. This theory does not account for capillary forces, which could be dominant at the size of the weld bead. Since it was first presented, no further work has expanded on this theory. Recently, Kumar and DebRoy[16] employed the Kelvin-Helmholtz instability theory to address similar geometries (not necessarily as a hydraulic jump mechanism) while accounting for surface tension.

Capillary instability humping model

The capillary instability humping model is based on Lord Rayleigh's theory of capillary instability of a free liquid cylinder.[18] His theory predicts that a small diameter liquid cylinder suspended in free space is unstable and will break up into a series of droplets. A series of beadlike protuberances evolve along the fusion line. Many researchers[2,8,9,11] include the instability of a free liquid cylinder model in their respective papers. Figure 6 is a representative model that includes the necessary parameters for predicting the critical length of instability. Gratzke[9] extends Rayleigh's model to account for a partially bounded liquid cylinder, which is a closer approximation to actual formation.

It is agreed that the BCM is owing to pure hydrodynamic effects. The most common situations for the BCM include high speed laser welding, electron beam welding and low current GMAW, where influence from arc pressure is low and a long cylindrical weld pool forms. It has also been noted to form under conditions

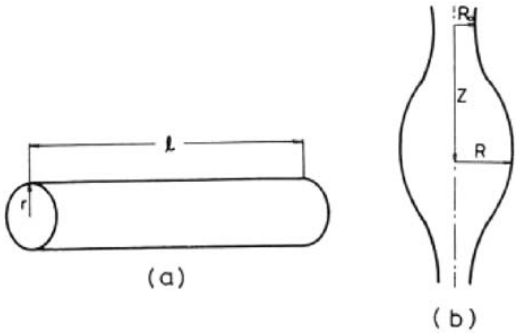

6 Model and parameters for predicting critical length for liquid instability[11]

other than welding, such as deposition of molten microdrops of wax.[12,19]

The dominating force under a flat welding condition is the surface tension of the molten metal. A liquid cylinder must form on the workpiece before humping. Figure 7 shows a schematic of the cross-section of a liquid cylinder resting on a plate and its parameters. The angle θ is highly dependent on the width of the weld pool and the amount of parent and filler metal melted.[20] Because the dominating force during BCM is the surface tension, the liquid cylinder preferentially separates into a series of beads if its length exceeds the critical length of instability. In this case, the driving force is minimisation of surface tension. Gratzke[9] has analysed the effects of gravity on welds in the flat position and has concluded that they are negligible. For out of position welds, however, gravity has a much greater influence.

Arc induced humping model

Paton[7] first suggested that a balance of pressure exists between the arc and the weld pool at normal welding rates. Arc pressure increases to the point of an imbalance in forces with increasing currents and defects begin to form. His arc force model was used to explain humping during SAW. In processes that use shielding gas, such as GTA and GMA welding, the pressure model needs to be revised. At currents exceeding 300 A, drag forces from the plasma are large enough to displace the majority of the molten weld pool directly below the arc. What is left is a thin layer of liquid metal referred to as the gouging region and a backfilled trailing region of metal. This process is illustrated in Fig. 8, taken from Shimada.[21] A rim of molten metal forms directly above the gouging region and acts as a channel for metal transfer, as shown in Fig. 1. The displaced metal is pushed into the trailing region of the weld and may subsequently form humps under favourable conditions. Mendez's force balance derivation[3] establishes a transition line that marks the change from the gouging region

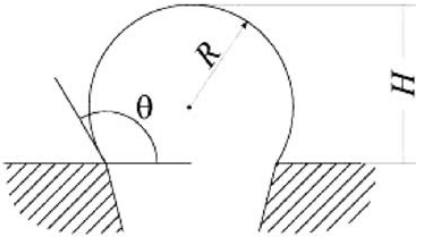

7 Cross-section of partially bounded liquid cylinder

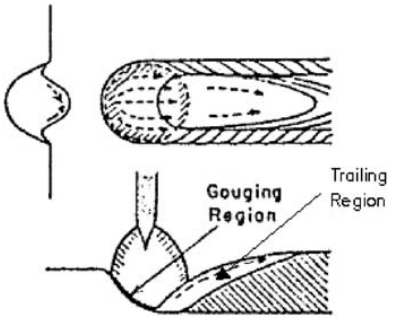

8 Schematic of arc induced humping model[18]

to the trailing region. The forces considered include the arc pressure, capillary pressure and the hydrostatic pressure of molten metal in the trailing region. His analysis continues by characterising each of these pressures and combining scaling relationships to finally derive a dimensionless equation that compares maximum pressure of the arc with maximum pressure of the molten metal. The critical value that determines the onset of humping in this relationship occurs when the arc pressure becomes larger than the metal pressure. In this situation, the arc has enough force to displace the molten metal out of the heat influence of the arc, an open gouging region forms, solidifies, and humping occurs. This model is referred to as the arc induced humping model because it is based on forces that originate from the arc. This model explains the GRM and experimental observations support this explanation.

Experimental observations

Many observations of these high speed welding defects have been made through experimentation. Bradstreet[2] was one of the first to report humping and tunnelling; and Nguyen[17] recently published his work on the humping process during GMAW. Other researchers[3–5,22] have all reported humping as it occurs during GTAW. Akahide[6] and Paton[7] demonstrated that humping forms during SAW. Albright[8] has reported it during laser welding. Even during electron beam welding, humping has been noted.[11] Throughout all of these studies, different welding parameters have been shown to significantly influence the formation of these high speed defects. The next section presents these parameters and attempts to explain their relationship with the two morphologies of humping.

Effect of welding parameters on beaded cylinder morphology

Power distribution

A limited amount of researches have been reported on humping as it occurs in laser and electron beam applications. Because these processes do not involve an electric arc, humping that does occur can be based primarily on the BCM as presented above. Albright[8] performed numerous laser beam welding experiments that produced several graphs similar to the one shown in Fig. 9. This is a basic map that delineates various regions of defects and the welding parameters used to create them. The experimental matrix consisted of both stainless and mild steels with varying thicknesses. The types of defect morphologies are consistent with the

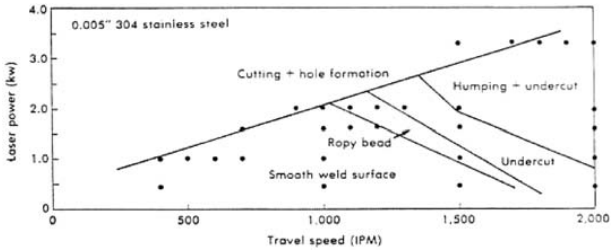

9 Plot showing various welding defects that form during laser welding and parameters used for formation[9]

BCM. Tsukamoto[11] showed that focal position has a large influence on the onset of humping during electron beam welding. As the beam focal point approaches the surface from below and the weld bead diameter decreases, humping occurs. When power density increased and the weld pool became narrower, humping was observed to occur more readily. Once the focal point rises above the surface, power density decreases, the pool widens and humping ceases. Tomie[10] performed similar electron beam welding experiments that implemented a tandem beam set-up that successfully curbed the formation of humps at high travel speeds. Owing to the fact that the power density decreases because power is distributed between two beams, humping is suppressed.

Shielding gas

The composition of the welding atmosphere has been shown to have a significant impact on humping. Bradstreet[2] experimented with various compositions of argon–oxygen shielding gas as well as pure carbon dioxide during GMAW. He noted that increasing levels of oxygen directly related to an increase in hump formation. In a carbon dioxide atmosphere, however, the onset of humping did not occur until the travel speed was three times that of the argon atmosphere. Nguyen[17] also noted similar results. Figure 10 shows the effects that different shielding gas can have on the onset of humping. Similar to Bradstreet, Nguyen showed that increasing the amount of carbon dioxide in the shielding gas would delay the onset of humping. Travel speeds can

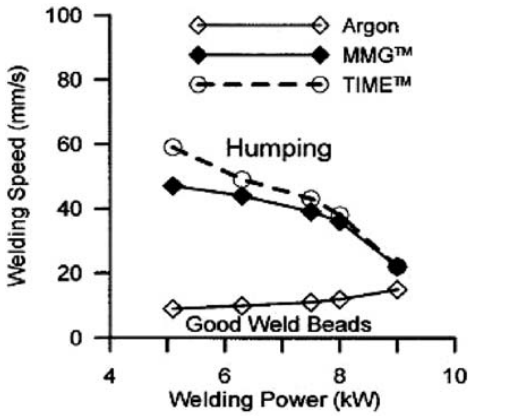

Shielding gas	Composition
Argon	100% Ar (Ultra High Purity Grade)
Mig Mix Gold™	92% Ar, 8% CO_2
TIME™	65% Ar, 8% CO_2, 26·5% He, 0·5% O_2

10 Effect of shielding gas on formation of humping defects in GMAW[16]

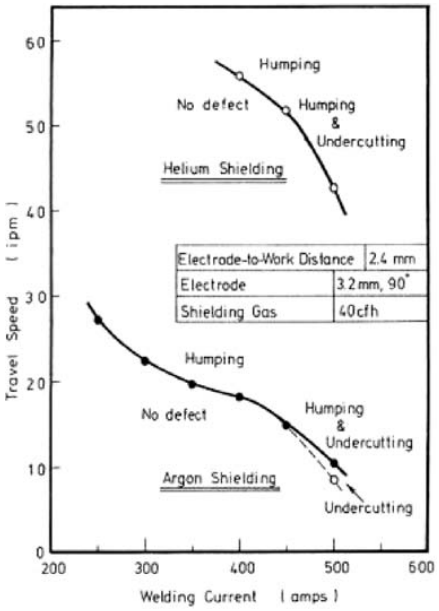

11 Effect of shielding gas on formation of humping defects in GTAW[4]

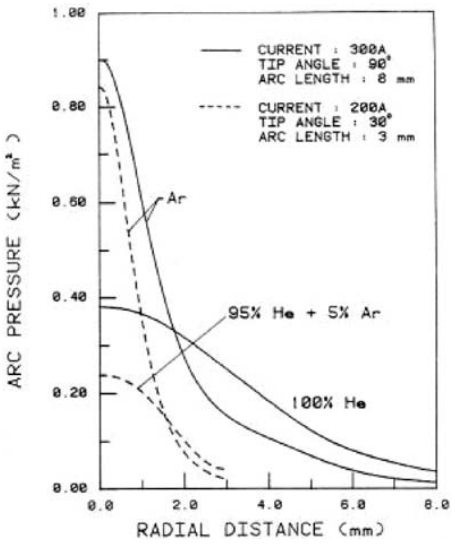

12 Effect of shielding gas on arc pressure distribution during GTAW[17]

be nearly five times as fast when using a gas blend as compared with pure argon. It is likely that this increase is owing to a change in the distribution of heat in the arc, which leads to a wider weld pool. Because the molten metal can spread out over a wider area, the formation of a liquid cylinder is less likely, and the BCM is hindered.

Surface tension

The flow of molten metal during welding is directly related to high speed welding defects. Bradstreet[2] noted that surface tension was expected to have a strong influence on the shape of a weld bead. He conducted a series of experiments that gradually increased the amount of oxygen in the argon shielding and attributed the changes in contact angles to changes in surface tensions and wetting. Other researchers[17,23–26] also believed that differences in bead morphology could be explained by variations in surface tension. Subramaniam[27] developed a technique for *in situ* measurements of the surface tension of molten steel droplets using a modified GMAW set-up and laser shadowgraphs. They were able to determine the effects of different shielding gases on the surface tension of steel. This research, however, did not explicitly determine the influence of shielding gas on weld bead morphology.

Other researchers believe that surface tension forces play a secondary role in bead morphology. Berezovskii[20] showed that actual wetting angles were extremely difficult to measure owing to the solidification interface found at the fusion line. In addition, he proposed that the weld bead morphology was governed primarily by the width of the weld pool, the amounts of melted base metal and the amount of filler metal deposited.

Trailing region

Nguyen[17] reported during GMAW that the filler metal droplets impinged on the gouging region and were redirected towards the trailing region. Figure 3*a–c* shows a weld produced in Nguyen's work that illustrates humping as it occurs in GMAW. Owing to the added volume of filler metal, a large swelling region forms and covers an open gouging region in GTAW. From the welding parameters used, the trailing region becomes long enough to satisfy the criteria presented in the capillary instability model and humping occurs due by BCM. Even though a gouging region is present, GRM does not occur owing to the lack of a premature freezing region ('dry spot' discontinuities between protuberances). In laser and electron beam welding, researchers[8,11] have reported similar elongated trailing regions. Owing to the lack of an arc in these processes, BCM is the mode of defect formation.

Effect of welding parameters on GRM

Arc force/pressure

Power distribution in laser and electron beam welding can be correlated to current and arc force distribution in arc welding. In the models that describe the GRM, the forces produced by the arc have a large influence on the onset of humping. Several researchers[4,28–32] performed experiments that measured various factors that contributed to changes in these arc forces. The following section will present the main factors that have been found to directly influence the suppression of humping.

Shielding gas

During GTAW, Savage[4] reported a large difference in the critical travel speed between argon and helium gas shielding as illustrated in Fig. 11. For a given current, the travel speed for the onset of humping almost tripled when switching from argon to helium, illustrating that helium gas delayed the onset of humping. Lin[30] has shown the pressure distribution produced in a gas tungsten arc changes significantly with the type of gas used as shown in Fig. 12. The reason for such a drastic difference is attributed to helium's lower density and higher viscosity at elevated temperatures. It is assumed the area that the pressure impinges upon correlates directly to the area of the heat spot, as mentioned above. At a given current, the total pressure acting on the weld pool is significantly less with helium shielding. Because the dominating force that governs the onset of the GRM

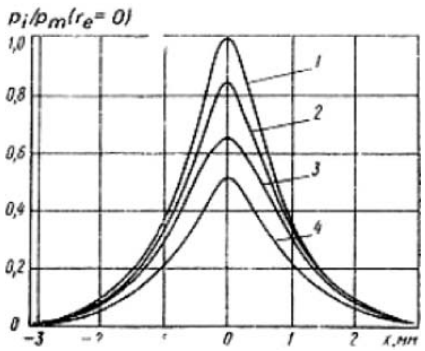

1 – 0 mm; 2 – 0·15 mm; 3 – 0·25 mm; 4 – 0·40 mm

13 Normalised pressure distribution for various radii of electrode truncation[31]

is pressure from the arc, currents need to be much higher with helium to produce sufficient force for humping.

Electrode geometry

Other factors that have been reported to change the pressure distribution during GTAW include the geometry of the tungsten electrode and the radius of electrode truncation. Several researchers[4,30,31] have all reported that a sharper electrode angle creates higher arc forces. Savage experimented extensively on the effect of electrode geometry, varying the diameters and vertex angles of the electrode tip. It is widely accepted that sharper tips create higher forces and therefore reduce the critical travel speed for humping. Selyanekov[31] varied the amounts of electrode truncation (blunting) and found that less truncation results in higher arc pressures. The results of this experiment are shown in Fig. 13. Blunter tips give lower peak pressures in the arc. Yamauchi[33] experimented with hollow electrodes and found a reduction in arc pressure as well. This reemphasises the fact that lowering arc pressures suppresses the onset of humping and results in faster travels speeds.

Metal composition

The base metal properties and alloy content can alter the formation of humped beads in several different ways. For example, the thermal conductivity of mild steel is roughly three times the value of stainless steel. Because mild steel can dissipate heat comparatively quicker than stainless steel, the former will tend to solidify faster than the latter, giving less time for the liquid cylinder to form and decreasing the likelihood of humping. Yamamoto[5] illustrated this concept experimentally. For a given travel speed, welding currents that caused humping in mild steel were nearly four times as high as the current in stainless steel. Differences in freezing range also affect the solidification time and tendency to hump.

Other researchers have studied the effects of surface active elements, mainly sulphur, and the role they play in humping. Mills[13] suggested that Marangoni flow could be strong enough to cause undercutting and humping, but they were unable to account for some occurrences. Mendez[3] observed no significant changes in penetration between high and low sulphur containing base metals during high current GTAW; however the amount of sulphur affected the critical humping speed and undercutting. In these cases, the geometry of the trailing

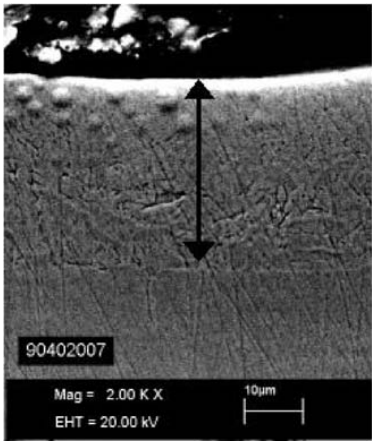

14 SEM image of solidified thin liquid layer formed in gouging region: arrows represent thickness of layer

region for higher sulphur steels was less 'wetting'. It is unclear, however, whether this was a direct effect of the surface tension, or an indirect effect of the disappearance of the side channels in the gouging region.

Gouging region

The thin liquid film and subsequent trailing regions described in the GRM have been thoroughly documented in experiments. Bradstreet[2] referred to it as a crater. Others[3,5,17] call it a gouging region. Mendez[3] and Pierce[34] have indicated that the driving force of this metal flow is aerodynamic drag produced from the arc. As explained above, this gouging region is one of the requirements for arc induced humping. Yamamoto[5] noted the thickness of the thin layer to be ~ 50 μm. When calculating the timescale for solidification, a typical value would be on the order of a few milliseconds. When this trailing region extends past the heat influence of the arc, solidification occurs instantaneously and trailing region is cut off from further accumulation. Figure 14 is the SEM image of the frozen gouging region showing a solidified layer of about 40 μm thickness. Extending these observations over the entire weld length will result in a series of humps that have interspaced sections of frozen gouging regions, as outlined in the GRM.

Prevention and mitigation of humping

In practical welding applications, several simple measures can be made to reduce or eliminate humping defects. As shown through experimental verification, twin electron beams made sound welds.[10] At the same travel speed, a single electron beam created humping. This practice should also reduce defect formation during GTAW. Other methods to reduce the GRM in GTAW include changing the electrode tip angle, truncating the tip, using a hollow electrode or switching to helium shielding gas. Nguyen[17] and Bradstreet[2] illustrated the drastic effects shielding gas composition can have on the limiting travel speed in GMAW. By switching to an argon/carbon dioxide mix, travel speeds may increase by up to 500%. Other tri gas and quad gas mixtures proved to be even more efficient. Owing to the greater expense of some of these mixtures, however, a cost benefit analysis would have to be performed for specific welding applications. In addition to cost differences, shielding

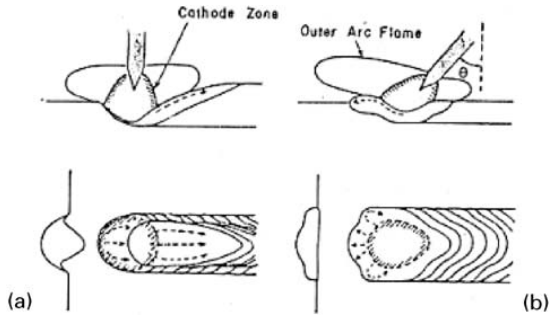

a $\theta=0^\circ$; *b* $\theta=45^\circ$

15 Typical bead formation during high current welding at different inclined torch angles[5]

gas composition will influence the penetration, reinforcement, contact angle, dilution, transfer modes, chemistry and properties of the weld. Understanding the benefits and shortcomings of changing welding parameters is critical. In many applications, travel speeds can be increased without drastically changing welding procedures.

Workpiece positioning can prevent humping by manipulating the flow of metal with gravity. Downhill welding angles have shown to increase the critical travel speed up to 25%.[17] Inclined torch angles have been shown to reduce the humping phenomenon as well.[5] Figure 15 illustrates how a forward inclined torch will change the metal flow and reduce the length of the molten tail.

Conclusions

The humping phenomenon has been shown to fall under two distinct classifications: GRM and BCM. Depending on the morphology of the defect, it was either created by the action of the arc on the liquid weld pool or by the capillary instability of a liquid cylinder. Several theories exist that attempt to explain defect formation, as presented above.

The GRM is formed because of forces produced by the arc that cause a gouging region to form directly under the electrode. This gouging region consists of a thin liquid film and the bulk of the molten metal is then pushed towards the rear of the weld pool. Humping occurs when the arc pressure extends the gouging region beyond the heat influence of the arc and premature freezing of the thin liquid film occurs. The backfilled trailing region then solidifies. The depth of penetration is independent of surface active elements, showing that Marangoni forces are not dominant. This type of humping can be reduced or eliminated by using a forward electrode angle, downhill welding, different shielding gas and a blunter or hollow electrode tip.

The BCM is typically observed with weld beads that are tall in relation to their width or in applications that cause a bead with a prominent dome and long molten tails. The driving force behind the BCM is the minimisation of surface energy by having a sequence of sphere like beads instead of a long smooth cylinder. This type of humping may occur with or without the presence of a gouging region and therefore penetration may or may not depend on Marangoni forces. Under similar welding conditions in different base metals, the molten metal tail is shorter in metals with higher thermal conductivity, therefore, the critical speed for humping is larger. For example, in GTAW of mild and stainless steels, the humping speed is higher in mild steel. Having a wider weld pool for the same deposition through changing the shielding gas can mitigate BCM. Besides, gravity forces during downhill welding oppose the capillary forces, which increase the critical travel speed.

Acknowledgement

The authors would like to gratefully thank the American Welding Society for providing funding for the present study.

References

1. ASM International: in 'ASM handbook', 1st edn, Vol. 6, 'Welding, brazing, and soldering', 1299; 1993, Materials Park, OH, ASM International.
2. B. J. Bradstreet: *Weld. J.*, 1968, **47**, (7), 314s–322s.
3. P. F. Mendez and T. W. Eagar: *Weld. J.*, 2003, **82**, (10), 296–306.
4. W. F. Savage, E. F. Nippes and K. Agusa: *Weld. J.*, **58**, (7), 1979, 212s–224s.
5. T. Yamamoto and W. Shimada: 'International symposium in welding', 1975, Japan Welding Society, Osaka, Japan.
6. K. Akahide: *Q. J. Jpn Weld. Soc.*, 1981, **50**, (12), 1165–1170.
7. E. O. Paton, S. L. Mandel'berg and B. G. Sidorenko: *Autom. Weld.*, 1971, **24**, (8), 1–6.
8. C. E. Albright and S. Chiang: *J. Laser Appl.*, 1988, **1**, (1), 18–24.
9. U. Gratzke, P.D. Kapadia, J. Dowden, J. Kroos and G. Simon: *J. Phys. D*, 1992, **25D**, 1640–1647.
10. M. Tomie N. Abe and Y. Arata: *Trans. JWRI*, 1989, **18**, (2), 175–180.
11. S. Tsukamoto, H. Irie, M. Inagaki and T. Hashimoto: *Trans. Natl Res. Inst. Met.*, 1983, **25**, (2), 8–13.
12. F. Gao and A. A. Sonin: *Proc. Roy. Soc. Lond. A*, 1994, **444A**, 533–554.
13. K. C. Mills and B. J. Keene: *Int. Mater. Rev.*, 1990, **35**, (4), 185–216.
14. M. L. Lin and T. W. Eagar: in 'Transport phenomena in materials processing', (ed. D. R. Poirier and G. H. Geiger), 1983, New York, ASME 63–69.
15. M. L. Lin and T. W. Eagar: *Weld. J.*, 1985, **64**, (6), 163–169.
16. A. Kumar and T. Debroy: 'Fabtech/AWS'; 2005, Chicago, IL, AWS.
17. T. C. Nguyen, D. C. Weckman, D. A. Johnson and H. W. Kerr: *Sci. Technol. Weld. Join.*, 2005, **10**, (4), 447–459.
18. L. Rayleigh: 'Theory of sound', Vol. 2; 1877, New York, Dover Publications.
19. S. Schiaffino and A. A. Sonin: *J. Fluid Mech.*, 1997, **343**, 95–110.
20. B. M. Berezovskii: *Autom. Weld.*, 1983, **36**, (10), 31–34.
21. W. Shimada and S. Hoshinouchi: *Q. J. Jpn Weld. Soc.*, 1982, **51**, (3), 280–286.
22. K. Ishizaki: 'Weld pool chemistry and metallurgy'; 1980, London, The Welding Institute.
23. K. Ishizaki: 'Physics of the welding arc'; 1962, London, The Institute of Welding.
24. A. Matsunawa and T. Ohji*: Trans. JWRI*, 1982, **11**, (2), 145–154.
25. A. Matsunawa and T. Ohji: *Trans. JWRI*, 1983, **12**, (1), 123–130.
26. A. Matsunawa: *Trans. JWRI*, 1984, **13**, (1), 147–156.
27. S. Subramaniam and D. R. White: *Metall. Mater. Trans. B*, 2001, **32B**, (2), 313–318.
28. S. H. Ko, D. F. Farson, S. K. Choi and C. D. Yoo: *Metall. Mater. Trans. B*, 2000, **31B**, 1465–1473.
29. I. V. Suzdalev and E. I. Yavno: *Weld. Prod.*, 1981, **28**, (11), 13–15.
30. M. L. Lin and T. W. Eagar: *Metall. Trans. B*, 1986, **17B**, 601–607.
31. V. N. Selyanenkov, V. V. Stepanov and R. Z. Saifiev: *Weld. Prod.*, 1980, **27**, (5), 6–8.
32. H. G. Fan and Y. W. Shi: *J. Mater. Process. Technol.*, 1996, **61**, (3), 302–308.
33. N. Yamauchi, T. Taka and M. Oh-I*: Sumitomo Search*, 1981, **25**, 87–100.
34. S. W. Pierce, P. Burgardt and D. L. Olson: *Weld. J.*, 1999, **78**, (2), 45–52.